ChemComm

Accepted Manuscript

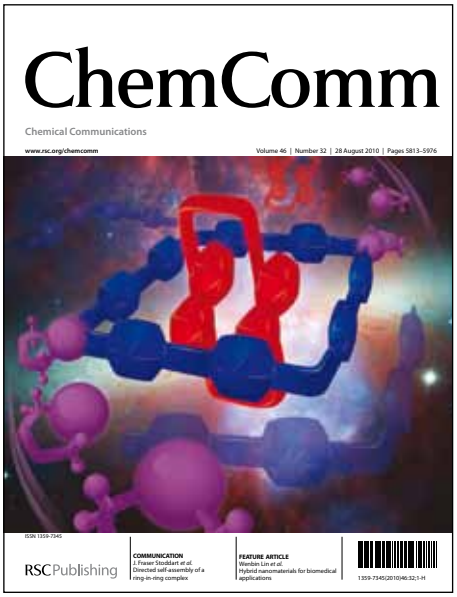

This is an *Accepted Manuscript*, which has been through the RSC Publishing peer review process and has been accepted for publication.

Accepted Manuscripts are published online shortly after acceptance, which is prior to technical editing, formatting and proof reading. This free service from RSC Publishing allows authors to make their results available to the community, in citable form, before publication of the edited article. This *Accepted Manuscript* will be replaced by the edited and formatted *Advance Article* as soon as this is available.

To cite this manuscript please use its permanent Digital Object Identifier (DOI®), which is identical for all formats of publication.

More information about *Accepted Manuscripts* can be found in the **Information for Authors**.

Please note that technical editing may introduce minor changes to the text and/or graphics contained in the manuscript submitted by the author(s) which may alter content, and that the standard **Terms & Conditions** and the **ethical guidelines** that apply to the journal are still applicable. In no event shall the RSC be held responsible for any errors or omissions in these *Accepted Manuscript* manuscripts or any consequences arising from the use of any information contained in them.

Cite this: DOI: 10.1039/c0xx00000x

www.rsc.org/xxxxxx

ARTICLE TYPE

Unusual pore structure and sorption behaviour in a hexanodal zinc-organic framework material

Jinjie Qian,[a,b] Feilong Jiang,[a] Linjie Zhang,[a,b] Kongzhao Su,[a,b] Jie Pan,[a,b] Qipeng Li,[a,b] Daqiang Yuan[a] and Maochun Hong*[a]

Received (in XXX, XXX) Xth XXXXXXXXX 20XX, Accepted Xth XXXXXXXXX 20XX

DOI: 10.1039/b000000x

A highly porous metal-organic framework structurally consists of three topological kinds of 3-connected 1,3,5-benzenetricarboxylate ligands, $Zn_2(COO)_4$, $Zn_3O(COO)_6$ and $Zn_4O(COO)_6$ SBUs, featuring a new 3,3,3,4,4,6-c hexanodal topology. Sorption behaviour in this complicated microporous MOF material has also been investigated.

Metal-organic frameworks (MOF) materials are recognized as a new subclass of solid state porous materials with high surface area and its tunable functional pore environment, which surpass significantly these commercially available materials such as activated carbons and zeolites in sorption capacity at ambient temperature, whose potential applications mainly focus on energy-related gas purification[1] and storage[2] to tackle the root of global climate problems, especially on-board hydrogen storage in mobile vehicles. More recently, great attention has been paid to the rational design and construction of microporous MOF materials owing to not only fascinating functions, but also aesthetic appeal.[3] Until now, large numbers of structural and topological types in the field of inorganic and organic compounds have been realized in coordination polymers and MOF materials,[4] however, building MOF materials with interesting structural and topological features reperesnets a huge challenge for chemists.

The structures of MOF materials are mainly made up of inorganic metal clusters and organic ligands, in which metal clusters are also known as the secondary building units (SBUs).[5] Generally speaking, it is the combination of both above components that decides the final framework topology, which in turn plays a key role in the final gas sorption behaviour as a storage adsorbent. Therefore, of particular interests are selecting the suitable SBUs and organic linkers for the proposed frameworks. Among typical SBUs, the dinuclear paddle-wheel clusters are the most commonly used ones in the isoreticular syntheses of MOF materials because they can easily generate lots of structures incorporating a wide range of organic ligands, for example HKUST-1.[6] However, in the crystal structure of Cr-MIL-101, $Cr_3O(CO)_6$ species are attached to the benzene dicarboxylate rings to result in a three-dimensional framework.[7] Last but not least, MOFs constructed from Zn_4O SBUs are quite common with extended organic ligands, such as MOF-5.[8] These known $M_2(O_2CR)_4$, $M_3O(O_2CR)_6$ and $M_4O(O_2CR)_6$ SBUs have been intensively utilized as square-planar, trigonal prismatic and octahedral SBUs by substitution of the available carboxylate groups. Although a large number of previously reported cases of MOFs contain one or two of them, such as CPM-5,[9] to pack all of them in one MOF material still remains great challenge.

Our group has been interested in the design and production of novel porous metal-organic materials.[10] We report herein the synthesis, single crystal structure and gas sorption behaviour of a new zinc-organic framework $[Me_2NH_2]_2[Zn_{10}(BTC)_6(\mu_3\text{-}O)(\mu_4\text{-}O)(H_2O)_5]\bullet 3DMA\bullet 9H_2O$ (denoted as **FJI-3**; H_3BTC = 1,3,5-benzenetricarboxylic acid; DMA = *N.N'*-dimethylacetamide) that integrates three types of SBUs components. Structurally speaking, it is constructed from three topologically different kinds of 3-connected BTC^{3-} ligands, featuring a new 3,3,3,4,4,6-c hexanodal net topology, whose gas sorption behaviour has also been investigated.

Colourless crystals of **FJI-3** are obtained under solvothermal reaction of H_3BTC ligands with $Zn(ClO_4)_2\cdot 6H_2O$ in a 1:1 molar ratio in an acidic (tetrafluoroboric acid, 40% in water) DMA solution at 100 °C for 5 days. The phase purity of the bulk product has been confirmed the powder X-ray diffraction (PXRD) analysis (Fig. S6). Single crystal X-ray diffraction analysis reveals that it crystallizes in the orthorhombic space group ***Ibam***. Its asymmetric unit contains seven independent Zn(II) ions and three BTC^{3-} ligands (BTC-1, BTC-2 and BTC-3), as shown in Fig. 1a. In coordination environment, these zinc ions adopt distorted tetrahedron ZnO_4 mode for Zn2, Zn5, Zn6, square pyramid ZnO_5 mode for Zn1, Zn4, Zn7, and octahedron mode for Zn3, respectively, with the observed Zn-O bond lengths in the range of 1.836(12) - 2.184(6) Å. As symmetry operation, both Zn1 and Zn7 can grow into dinuclear zinc paddle-wheel SBUs (PW1 and PW2) where PW1 is assembled by BTC-1 and BTC-2, while PW2 only by BTC-3. Zn2 and Zn3 link together to give an unusual Zn_3O SBU, where Zn2 is monodentated by one carboxylate oxygen atom from BTC-1, and Zn4, Zn5 and Zn6 link together to give a Zn_4O SBU (Fig. 1b).

It should be noted that two of three carboxylate groups in BTC-1 adopt a chelating mode to link PW1 and Zn_4O SBU, while the left one takes a monodentating mode to link Zn_3O SBU (Fig. S3). However, all of the carboxylate groups in both BTC-2 and BTC-3 ligands adopt a chelating mode where the BTC-2 is connected to PW1, Zn_3O and Zn_4O SBU, while the BTC-3 is connected to PW2, Zn_3O and Zn_4O SBU. PW1 and PW2, typical dinuclear zinc paddle-wheel units, both serve as 4-c nodes. As depicted in Fig 1b, the Zn_3O SBU is unlike the typical characteristic of the $M_3O(O_2CR)_6$ building block which usually is the junction of the three octahedral by sharing a μ_3-O atom. In this 6-c Zn_3O SBU, Zn2 ion is in 4-coordinated tetrahedral geometry, while Zn3 ion is typically 6-coordinated with one terminal coordinated water molecule.

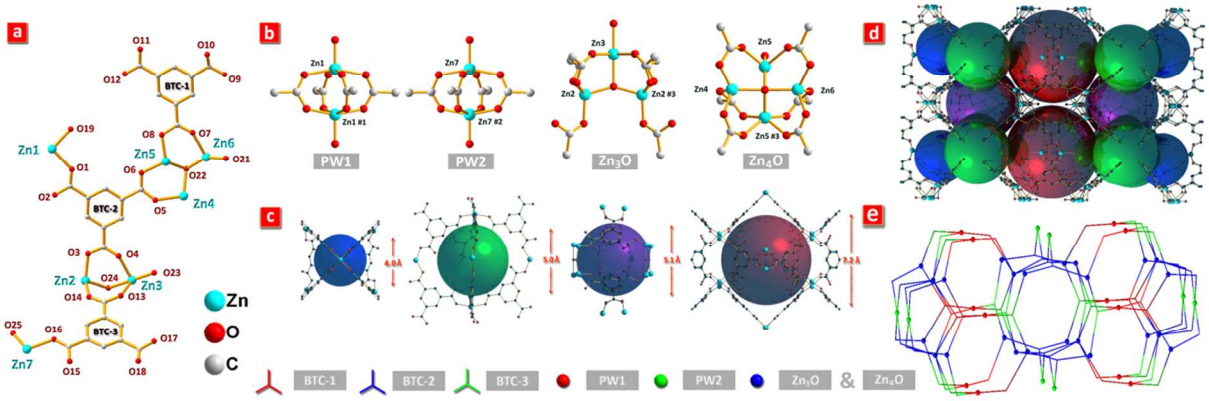

Fig 1. a) The asymmetric unit of **FJI-3**; b) Secondary building units, symmetry codes: #1 = 1-x, y, 0.5-z; #2 = -x, 1-y, z; #3 = x, y, 1-z.; c) Four kinds of cages; d) Schematic of pore framework structure for **FJI-3**; e) Topological representation of **FJI-3**.

Although these Zn_4O SBUs similarly act as 6-c nodes, the coordination environments for Zn atoms are different from typical $M_4O(O_2CR)_6$ SBU, in which four Zn atoms have same four-coordinated tetrahedral geometries by sharing a μ_4-O atom.

Careful examination of **FJI-3** shows us that it is a three-dimensional framework with a very complicated solvent pore structure. There are four kinds of microporous cages with different sizes ranging from 4.0 ~ 7.2 Å (Fig 1c and S4). From topological viewpoints, the BTC^{3-} ligands serve as three kinds of 3-c nodes, whereas PW1 and PW2 as two kinds of 4-c nodes, Zn_3O and Zn_4O SBUs are one kind of 6-c nodes (ESI, section S4). As a consequence, **FJI-3** adopts a very rare 3,3,3,4,4,6-c 6-nodal network with topological point symbol of $\{4.6\text{^}2\}_4\{4.8\text{^}2\}_8\{4\text{^}3.6\text{^}4.8\text{^}8\}_4\{6\text{^}2.8\text{^}4\}\{8\text{^}6\}_2$ (Fig. 1e), which is previously never reported in the field of MOF materials. Finally, we notice that the distorted $Me_2NH_2^+$ cations lie inside the large solvent accessible void, which is the byproduct of *in situ* decomposition of the DMA solvent, thus leading to the charge equilibrium.[11]

The free volume of **FJI-3** with removal of guest solvent molecules is calculated to be ~57.8% by PLATON and the calculated pore volume is 0.29 $cm^3\ g^{-1}$. We find that **FJI-3** well retains its framework in acetonitrile which is confirmed by the following PXRD test. The permanent porosity has been confirmed by the obtained N_2 adsorption isotherm at 77 K. The desolvated sample exhibits a reversible type I N_2 isotherm, which confirms retention of microporosity upon removal of guest solvent with saturated uptake of 187 $cm^3\ g^{-1}$ at 77 K (Fig. 2a). As one of microporous materials, **FJI-3** corresponds to BET and Langmuir surface area of 697 $m^2\ g^{-1}$ and 800 $m^2\ g^{-1}$, respectively. A pore size distribution analysis conducted by Horvath-Kawazoe method shows that there is a wide distribution of micropores at 0.4 ~ 1.2 nm with the maximum distribution centered at ~0.5 nm, which accords well with the internal structural features of cages.

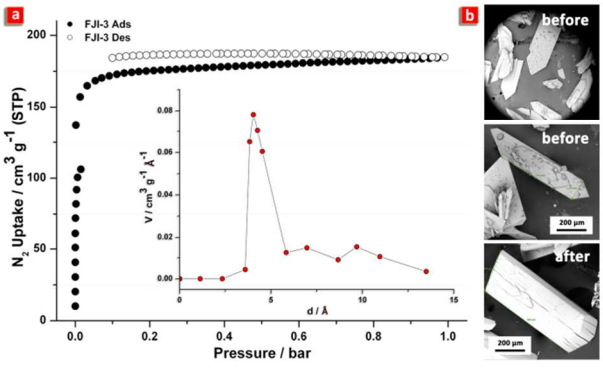

Fig. 2 a) Experimental N_2 isotherms for **FJI-3** at 77 K, ● adsorption, ○ desorption. Inset shows the pore size distribution dV/dw (*V*) vs. pore width (*d*); b) SEM images before and after the activation process.

Meanwhile, we also investigate volumetric H_2 uptake in **FJI-3** at 77 K and 87 K. All H_2 isotherms show rapid kinetics and good reversibility without hysteresis (Fig. 3a). The H_2 uptake capacity is up to 141.3 $cm^3\ g^{-1}$ (1.26 wt %) at77 K and 1.0 bar, and 101.3 $cm^3\ g^{-1}$ (0.91 wt %) at 87 K and 1.0 bar. These absolute values in hydrogen capacity are quite comparable with those of recently reported highly porous MOF materials at the same condition.[13] Moreover, the adsorption heat of hydrogen (Q_{st}) is simulated by the Clausius-Clapeyron quation and its value at zero coverage for **FJI-3** is calculated to be 4.16 kJ mol^{-1}, and increases slowly with incessant H_2 loading (Fig. 3b), much lower than those of many famous porous materials, such as FJI-1 (4.62 $kJ.mol^{-1}$), MOF-5 (5.2 kJ mol^{-1}), NOTT-122 (6.0 kJ mol^{-1}), HKUST-1 (6.6 kJ mol^{-1}) and FJI-2 (7.18 kJ mol^{-1}),[4c,6,8,10b] In this case, we consider that the high H_2 uptake capacity is decided by the instrinsicly large guest-accessible volume,

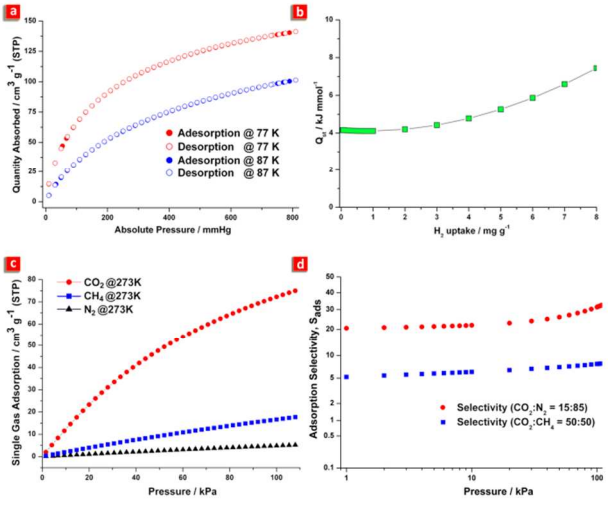

Fig. 3 a) H_2 isotherms for **FJI-3** at 810 mmHg and 77 K; b) The adsorption heat of H_2 for **FJI-3**. (c) CO_2, CH_4 and N_2 uptake curves at 273 K. (d) Adsorption selectivity of CO_2 over CH_4 or N_2.

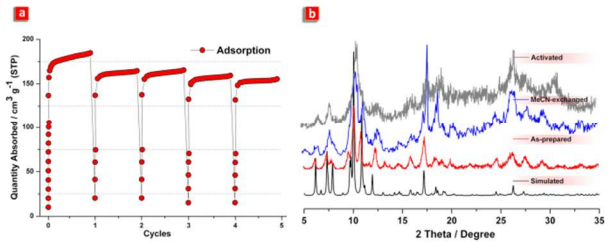

Fig. 4 a) Cycles of N_2 uptake at 77 K; b) PXRD patterns simulated: from the cif (black); from the as-obtained sample (red), from the MeCN-exchanged sample (blue), from the desolvated sample (gray).

while the lower binding affinity might be attributed to its interlinked cage-based interior or incomplete activation.

The special cage-based large space in **FJI-3** inspires us to further explore the potential functionalities toward CO_2/CH_4 and CO_2/N_2 gas separation. In this case, single component low pressure gas sorption isotherms toward CO_2, CH_4 and N_2 at 273 K are recorded and presented in Fig. 3c. Some deficiencies can be observed for CO_2 uptake in adsorption isotherm, specificly in very low relative pressure (0.10 bar, 12.3 $cm^3\ g^{-1}$), whose CO_2 isotherm displays a very flat slope, however, good materials tend to show a rapidly steep slope in low relative pressure zone. While at 273 K and 1.0 bar, the maxmium uptake of CO_2 is 72.2 $cm^3\ g^{-1}$, even a little bit higher than that of FJI-2 (71.6 $cm^3\ g^{-1}$) at the same conditions, which is also comparably much higher than these obtained values of CH_4 and N_2 isotherms, as shown in Fig. 3c. CH_4 uptake of **FJI-3** at ambient pressure is just 17.7 $cm^3\ g^{-1}$ at 273 K and 10.5 $cm^3\ g^{-1}$ at 295 K, and N_2 uptake is just 5.2 $cm^3\ g^{-1}$ at 273 K and just 3.3 $cm^3\ g^{-1}$ at 295 K. Thus compared to CO_2 at the same condition, these much lower uptake of CH_4 and N_2 encourages us to investigate the selectivity. Therefore, we try to predict binary mixture adsorption selectivity by adopting the ideal adsorbed solution theory (IAST)[13]. Utilizing the pure component isotherm fits, the adsorption selctivity is defined by $S_{ads} = (q_1/q_2)/(p_1/p_2)$, where q_i is the amount of i adsorbed and p_i is the partial pressure of i in the mixture. This material shows a very high $S_{ads}(CO_2/N_2)$ of ~32.5 in a 15:85 molar ratio of CO_2 and N_2 mixtures at 273 K and 1.0 bar, indicating that this material may be a promising candidate for post-combustion CO_2 capture application. Moreover, the calculated CO_2/CH_4 selectivity tatio is up to ~7.9 at 273 K and 1.0 bar from equimolar gas-phase mixtures (Fig. 3d), which is comparable to the high selectivities of CO_2 over CH_4 in reported $Cu(bpy\text{-}n)_2(SiF_6)$.[14] Thus, the high selectivity of CO_2/CH_4 at ambient pressure potentially makes it useful for future natural gas purification.

In following sorption experiment, we try to verify the cyclability of desolvated material for practical application by loading them on an ASAP2020 analyzer. We record the five cycles of N_2 adsorption at 77 K without the reactivation process between cycles. There is a very slight loss in absorbed quantity for **FJI-3** after 5 cycles, especially between the firtst two cycles (Fig. 4a). A ~10.6% loss (1st cycle, 184.3 $cm^3\ g^{-1}$; 2nd cycle, 164.7 $cm^3\ g^{-1}$) can obviously be observed at the first two cycles, but no apparent adsorbed quantity loss can be found (3rd cycle, 165.5 $cm^3\ g^{-1}$; 4th cycle, 159.4 $cm^3\ g^{-1}$, 5th cycle, 155.5 $cm^3\ g^{-1}$), thus indicating incomplete desorption during each generation cycle without reactivation process. Despite good gas uptake capacity, the regeneration energy penalty is inevitably required for **FJI-**3 to renew an active material for future applications.

This work was financially supported by the 973 Program (2013CB933203; 2011CBA00507), National Nature Science Foundation of China (21131006), and the Nature Science Foundation of Fujian Province.

Notes and references

[a]*Key Laboratory of Coal to Ethylene Glycol and Its Related Technology, State Key Laboratory of Structure Chemistry, Fujian Institute of Research on the Structure of Matter, Chinese Academy of Sciences, Fuzhou, Fujian, 350002, China*
[b]*Graduate School of the Chinese Academy of Sciences, Beijing, 100049, China*
**To whom correspondence should be addressed: E-mail:hmc@fjirsm.ac.cn; Fax: +86-591-83794946; Tel: +86-591-83792460*

Crystal data for **FJI-3**: $C_{27}H_9O_{22}Zn_5$, M_r = 1012.19, light yellow, 0.12 × 0.08 × 0.04 mm^3, orthorhombic, space group ***I***bam (No. = 72), a = 19.7757(2) Å, b = 44.7064(5) Å, c = 28.6303(3) Å, V = 25312.1(5) $Å^3$, T = 173(2) K, Z = 16, D_c = 1.062 g cm^{-3}, λ = 0.71073 Å, $2\theta_{max}$ = 65.0°, F(000) = 7952, GOF = 1.072, R_1 and wR_2 are 0.0850 and 0.2709, respectively. CCDC No. 967656. Finally, the topology of the network is analyzed by the program package TOPOS.[15]

1 (a) McDonald, T. M.; Lee, W. R.; Mason, J. A.; Wiers, B. M.; Hong, C. S.; Long, J. R. *J. Am. Chem. Soc.* **2012**, *134*, 7056. (b) Qian, J. J.; Jiang, F. L.; Yuan, D. Q.; Wu, M. Y.; Zhang, S. Q.; Zhang, L. J.; Hong, M. C. *Chem. Commun.* **2012**, *48*, 9696.
2 (a) Lu, W. G.; Yuan, D. Q.; Makal, T. A.; Li, J. R.; Zhou, H. C. *Angew. Chem. Int. Ed.* **2012**, *51*, 1580. (b) He, Y. B.; Xiang, S. C.; Zhang, Z. J.; Xiong, S. S.; Wu, C. D.; Zhou, W.; Yildirim, T.; Krishna, R.; Chen, B. L. *J Mater Chem A* **2013**, *1*, 2543.
3 (a) Zhou, K.; Jiang, F. L.; Chen, L.; Wu, M. Y.; Zhang, S. Q.; Ma, J.; Hong, M. C. *Chem. Commun.* **2012**, *48*, 12168.
4 (a) Lu, W. G.; Yuan, D. Q.; Makal, T. A.; Li, J. R.; Zhou, H. C. *Angew. Chem. Int. Ed.* **2012**, *51*, 1580. (b) Zheng, S. T.; Wu, T.; Zuo, F.; Chou, C. S.; Feng, P. Y.; Bu, X. H. *J. Am. Chem. Soc.* **2012**, *134*, 1934. (c) Qian, J. J.; Jiang, F. L.; Su, K. Z.; Pan, J.; Zhang, L. J.; Li, X. J.; Yuan, D. Q.; Hong, M. C. *J Mater Chem A* **2013**, *1*, 10631.
5 Rosi, N. L.; Kim, J.; Eddaoudi, M.; Chen, B. L.; O'Keeffe, M.; Yaghi, O. M. *J. Am. Chem. Soc.* **2005**, *127*, 1504.
6 Chui, S. S. Y.; Lo, S. M. F.; Charmant, J. P. H.; Orpen, A. G.; Williams, I. D. *Science* **1999**, *283*, 1148.
7 Ferey, G.; Mellot-Draznieks, C.; Serre, C.; Millange, F.; Dutour, J.; Surble, S.; Margiolaki, I. *Science* **2005**, *309*, 2040.
8 J. L. C. Rowsell, A. R. Millward, K. S. Park and O. M. Yaghi, *J. Am. Chem. Soc.*, **2004**, *126*, 5666;
9 Zheng, S. T.; Bu, J. T.; Li, Y. F.; Wu, T.; Zuo, F.; Feng, P. Y.; Bu, X. H. *J. Am. Chem. Soc.* **2010**, *132*, 17062.
10 (a) Shan, X. C.; Jiang, F. L.; Yuan, D. Q.; Zhang, H. B.; Wu, M. Y.; Chen, L.; Wei, J.; Zhang, S. Q.; Pan, J.; Hong, M. C. *Chem. Sci.* **2013**, *4*, 1484. (b) Han, D.; Jiang, F. L.; Wu, M. Y.; Chen, L.; Chen, Q. H.; Hong, M. C. *Chem. Commun.* **2011**, *47*, 9861. (c) Qian, J. J.; Jiang, F. L.; Yuan, D. Q.; Li, X. J.; Zhang, L. J.; Su, K. Z.; Hong, M. C. *J Mater Chem A* **2013**, *1*, 9075.
11 (a) Zheng, S. T.; Wu, T.; Zuo, F.; Chou, C. S.; Feng, P. Y.; Bu, X. H. *J. Am. Chem. Soc.* **2012**, *134*, 1934.
12 (a) H. Hayashi, A. P. Côte· , H. Furukawa, M. O'Keeffe, O. M. Yaghi, *Nat. Mater.*, **2007**, *6*, 501. (b) Park, K. S.; Ni, Z.; Cote, A. P.; Choi, J. Y.; Huang, R. D.; Uribe-Romo, F. J.; Chae, H. K.; O'Keeffe, M.; Yaghi, O. M. *PNAS* **2006**, *103*, 10186.
13 (a) J. An, S. J. Geib and N. L. Rosi, *J. Am. Chem. Soc.*, **2010**, *132*, 38. (b) A. L. Myers and J. M. Prausnitz, *AIChE J.* **1965**, *11*, 121.
14 (a) S. D. Burd, S. Ma, J. A. Perman, B. J. Sikora, R. Q. Snurr, P. K. Thallapally, J. Tian, L. Wojtas, M. J. Zaworotko, *J. Am. Chem. Soc.* **2012**, *134*, 3663.
15 V.A. Blatov, *IUCr Compcomm Newsl.*, **2006**, 7, 4.